

A Novel Approach for Islanding Detection in Distributed Generation Systems Using the 3-Parameter Sine Fit Algorithm to Improve Power System Reliability

Sudheeksha Misra¹, Bhola Jha^{2,*}, and V. M. Mishra²

ARTICLE INFO

Article history:

Received: 18 December 2023 Revised: 19 May 2024 Accepted: 29 June 2024 Online: 31 October 2025

Keywords: ROCPAD Islanding ROCOF 3PSF Reliability

ABSTRACT

The false detection of islanding affects the working personnel, grid stability, and power system reliability, which require corrective action. An accurate islanding detection algorithms, voltage management techniques, and improved system resilience are needed to mitigate these concerns. In continuation, an innovative approach to islanding detection that makes use of the 3 Parameter Sine Fit (3PSF) technique has been introduced, that calculates the voltage-current angle at the Distributed Generators (DG) location. The proposed method enhances the islanding recognition accuracy of an adapted microgrid test system comprising an Emergency Diesel Engine Generator (EDEG) and three Wind Energy Generators (WEG). To illustrate the effectiveness of the recommended novel method, the evaluation is performed under various conditions, like islanding in low as well as in high power mismatching, short circuit fault, and voltage sag-swell at different percentages of nominal voltage. The comprehensive evaluation serves as a testament to the efficacy and robustness of the proposed method. It also illustrates resiliency and reliability under various percentage voltage settings. The MATLAB results are thus obtained and compared to ROCOF, and it has been noted that the suggested approach overcomes the sensitivity and reliability of the test system.

1. INTRODUCTION

Present-day power systems must have the capability to deal with extreme intricacy and sensibility Among the traits of contemporary grids related to the extension of upcoming electricity systems represent the significant involvement of DGs within the system, which have several issues, such as the reliability of power systems which depends on accurate voltage sag and swell measurement, good fault management, and effective islanding identification. During outages, islanding detection protects against isolated grid segments, guaranteeing both system stability and worker safety. In order to maintain a steady power supply and avoid interruptions or damage to delicate equipment, monitoring voltage variations such as sags and swells is essential. Fault management prevents power outages and malfunctioning equipment by quickly identifying and resolving them.

These components work together to provide a dependable power system that is stable, resilient, and therefore able to serve industries and consumers. The crucial requirement for DGs in distribution systems is islanding detecting capability. According to various technical manuals, all DG must be automatic unplugged after a grid failure and must stay detached until the regular grid supply is reinstated. Islanding needs to be identified in fewer than two seconds, as per IEEE

1547 [1]. Local and distant islanding detection methods are the two main categories. The lines that connects the DG and PCC are employed in the remote approach, such as transfer trip relaying [2], [3]. Microprocessor systems [4], power line cable communication (PLCC) [5, 6], supervisory control and data acquisition (SCADA), and in [6], power line signaling is utilized to identify islanding through transmission a short signal that travels along the DG bus and reaches the breaker site. Islanding identification in [7] is achieved by the application of morphological filtering and breakdown of empirical codes.

This is anticipated that the identification speed is slow due to the sluggish nature of filter quality. Islands inside the restricted non-detection zone (NDZ) can be located using remote detection techniques.

These methods are also quick at identifying islanding situations and separating islanding from disruptions associated with the grid. The main drawbacks of remote techniques are that they can be costly and challenging to implement, and there's a chance that the communication link will fail. They also require backup protection.

Local approaches can be classified as either active or passive. To consciously find the islanding conditions in the running operations, an intentional interruption is introduced

¹Department of Electrical Engineering, VMSBUTU, Dehradun, GBPIET, Pauri Garhwal.

²Department of Electrical Engineering, GBPIET, Pauri Garhwal, VMSBUTU, Dehradun.

^{*}Corresponding author: Bhola Jha; Email: bjhallfee@gbpiet.ac.in.

into the framework. Thus, the active methods are used for a certain DG, such as an inverter-based DG. Additionally, the system is not updated with the disturbance signal via the DG in the active approaches. Therefore; It is possible to intentionally create equality power imbalances by adding a condenser or capacitor by [8], [9] in order to find an islanding condition.

Some of the active procedures for DGs, that are inverterbased include the active frequency drift [10], the current harmonic injection by [11], the Sandia frequency shift by [12], the positive feedback technique by [13], and the voltage drifting approach by [14]. Selectively few components of high-frequency injected current are a difficulty for the current injection approach for islanding used in [15]. For synchronous-based generators, comparable islanding discovery methods are given in [16–18]. In [16], two active and reactive power control loops using positive feedback are available to make the unreliable system unstable in the event of an islanding. . Subsequently, new loops for both active and passive power regulation were proposed in [18], which improve the synchronous generator's capacity to recognise islanding conditions and ride over obstacles. In order to introduce some instability within the system during islanding, the [17] additionally incorporates synchronous generator excitation mechanism and inherent controllers to the governor. A method for controlling the two probabilistic phasing neural network controllers is described in [19].

The Active approaches may obstruct non-linear loads and other tools that introduce disruptions into the set-up. The deterioration of the electrical quality is another disadvantage of active islanding strategies.

Passive techniques start with monitoring the electrical values in the system. Passive approaches have the advantage of not affecting the usual functioning of the DG system when they are adopted. However, active strategies add an outside disruption to the output of the inverter, which lowers the power characteristics even if they typically possess a quicker reaction time and a smaller NDZ than passive technique. Techniques for detecting passive islanding is suitable for both inverter-based and synchronous (DGs). Choosing the most crucial factor and its cutoff point for determining islanding while minimizing annoyance tripping is the key issue in using a passive islanding detection system. Present in [20], relays with frequency or over/under voltage are the most often used passive detecting devices. One of the widely used techniques for detecting islanding is the ROCOF, which has a large NDZ. Another is the vector surge relays that were introduced in [21], which use the wavelet transform to detect islanding and decrease NDZ. Other passive technologies that have recently been introduced in [22] are other examples using high-frequency impedance monitoring and near-loop frequency control, [23] and [24] presented a passive method regarding DGs rooted in the inverter. A voltage index was employed in [25]

to ascertain the islanding condition for large power differentials. The line current was checked for small power disparities to unplug particular components since small imbalances might cause large power mismatches. PCC voltage is broken down into a number of oscillatory components in [26] using the modified empirical mode decomposition (EMD) technique in order to identify islanding. Learning strategies are developed in [27] to determine the characteristics that set islanding apart from the grid connected situations. Initial feature analysis utilizing signal processing techniques is followed by a deep learningbased strategy for classifying islanding and grid-linked interruptions. In [28], islanding is detected by dividing the negative sequence voltages by the current of both the grid and the DG. In [29], a modal current and adaptive boosting method is proposed. The modal current is transformed into a current's nano-frequency component using the EMD tool, and these currents are then correlated to identify islanding with the use of Hilbert's transform. A novel technique to identify islanding using logical operators is presented in [30], yet it does not illustrate how islanding affects other DG or how line loss occurs. Compared to the older technique, the current ROCPAD method [31] detects islanding with more accuracy. In [31], islanding is thoroughly examined regarding power imbalances between 0% to 80% and the paper [32] presents a nonlinear modeling of system identification approach for securing distributed generatorbased inverters from islanding. Some of the study is also done in the area of management of energy in case of islanding the paper [33] and [34] discussed the same.

This study proposes an innovative method, the 3PSF technique, to calculate the angle for the passive islanding identification method ROCPAD and contrast it to ROCOF. These are employed in the islanding recognition of faults and voltage sag-swell condition.

The following are the suggested method's primary contributions:

- It instantaneously detects the islanding without any delay.
- The proposed method recognizes islanding when there is a 0% power mismatch.
- The test system integrated with maximum DGs can be simulated without compromising the system's reliability.
- It is based on widely-used protective relays; and implemented with ease.
- The suggested method can identify islanding under voltage sag-swell conditions.

Further, the arrangement of the paper is as follows. The literature review is already been discussed in Section 1. Section 2 provides an outline of the problem statement and the suggested methodology. An overview of the test system in brief and Sections 3 and 4 offer a discussion of the

findings, respectively. At last, the paper concludes with scopes for future work in Section 5.

2. PROPOSED METHODOLOGY

The inadequate detection of islanding can have dangerous repercussions such as unintentional energizing systems that might endanger the safety of worker, uncontrolled voltage and frequency fluctuations that could harm equipment, and unstable grid conditions. Voltage sags and swells exacerbate system problems by causing device failure, disruptions in operations, and reduced power quality. Sags may cause equipment to fail or shut down, while swells can cause stress on components, which can lower customer satisfaction. On the other hand, false islanding detections provide a unique set of challenges as they trigger needless safeguards that interfere with distributed generation systems and may result in service disruptions and unstable grids. Altogether these mistakes affect overall grid stability and reliability which require corrective action. To mitigate these concerns, accurate islanding detection algorithms, voltage management techniques, and improved system resilience are needed.

The 3PSF is employed in the suggested technique, which is dependent on the parameter approximation. Equal interval samples are taken from a sine function signal model to produce a sine function expression, The sample sequence is fitted utilizing the least squares method to estimate the frequency, sine-wave's amplitude, DC component and phase.

To find the phase angle of the signal.

Let us examine the signal found in eqn. (1).

$$y = E\sin(wt + \varphi) + c \tag{1}$$

where

y is the voltage signal

E is the signal's amplitude

w is the frequency of angular motion.

 ϕ is the angle of phase.

One can expand eqn. (1) to eqn. (2):

$$y = E \sin w t \cos \phi + E \cos w t \sin \phi \tag{2}$$

&
$$y = E_1 \sin wt + E_2 \cos wt$$

where:

$$E_1 = E \cos \emptyset \tag{3}$$

$$E_2 = E sin\emptyset (4)$$

One may get eqn. (5) from eqns. (3) and (4).

$$E = \sqrt{E_1^2 + E_2^2} \tag{5}$$

Eqn. (6) may be used to obtain the phase angle \emptyset .

$$\emptyset = \left\{ \begin{aligned} & \arctan \frac{-E_1}{E_2}; E_2 \ge 0 \\ & \arctan \frac{-E_1}{E_2} + \pi; E_2 \ge 0 \end{aligned} \right\}$$
 (6)

Since the sequence time is t_1 , t_2 t_n and the respective data are y_1 , y_2 y_n . The sum-squared fit error between function fitting values and eqn.(7) illustrates how sample data is represented in the fitting method.

$$f(abc) = \sum [y_i - (E_2 coswt + E_1 sinwt + c)]^2$$
(7)

The requirement indicated in eqn. 8 must be met in order to minimize the error.

$$\frac{\partial f}{\partial E_1} = 0; \frac{\partial f}{\partial E_2} = 0; \frac{\partial f}{\partial c} = 0 \tag{8}$$

The eqn. 9 may be expressed as

$$\sum y_i - \sum E_2 coswt - \sum E_1 sinwt - \sum c$$
 (9)

&
$$\sum E_2 coswt + \sum E_1 sinwt + \sum c = \sum y_i$$
 (10)

Let: $a_i = coswt$

 $b_i = sinwt$

Next, the following calculations are made using eqn. 11to 14 to get E1 and E2, and the value of \emptyset is determined using the results of those calculations.

$$E_2 \sum a_i^2 + E_1 \sum a_i b_i + c \sum a_i = \sum y_i a_i$$
 (11)

$$E_2 \sum a_i b_i + E_1 \sum b_i^2 + c \sum b_i = \sum y_i b_i$$
 (12)

$$E_2 \sum a_i + E_1 \sum b_i + c \sum 1 = \sum y_i \tag{13}$$

The aforementioned eqn. (11), (12), and (13) may be expressed as a matrix.

$$A.B = X \tag{14}$$

here,

$$A = \begin{bmatrix} \sum_{i=1}^{n} a_i^2 & \sum_{i=1}^{n} a_i b_i & \sum_{i=1}^{n} a_i \\ \sum_{i=1}^{n} a_i b_i & \sum_{i=1}^{n} b_i^2 & \sum_{i=1}^{n} b_i \\ \sum_{i=1}^{n} a_i & \sum_{i=1}^{n} b_i & \sum_{i=1}^{n} 1 \end{bmatrix}$$

$$\mathbf{B} = \begin{bmatrix} E_2 \\ E_1 \\ c \end{bmatrix} \qquad ; \mathbf{X} = \begin{bmatrix} \sum_{i=1}^n y_i . \ a_i \\ \sum_{i=1}^n y_i . \ b_i \\ \sum_{i=1}^n y_i \end{bmatrix}$$

The current waveform is then subjected to the same process, which yields the current angle.

The ROCPAD is then computed using eqn. 15.

$$ROCPAD = \frac{d(\emptyset_v - \emptyset_i)}{dt}$$
 (15)

The next crucial step is to figure out the frequency for ROCOF. Thus, the sine signal represented in eqn. 16 may be expressed as:

$$y_i = Esin(\theta_i + \emptyset) + c \tag{16}$$

where, $i = 1, 2, \dots, n$.

&
$$\theta_i = \frac{2\pi i}{N}$$

The eqn. (17) can then be obtained.

$$y_i = Esin\left(\frac{2\pi i}{N} + \emptyset\right) + c \tag{17}$$

The frequency is calculate by lissajous technique and then from eqn. 18. The ROCOF is calculated.

$$ROCOF = \frac{df}{dt} \tag{18}$$

The calculated ROCOF is contrasted with the predefined threshold value. When the value of islanding exceeds the predefined threshold limit, islanding is identified. The ROCOF technique flowchart is shown in Fig. 1.

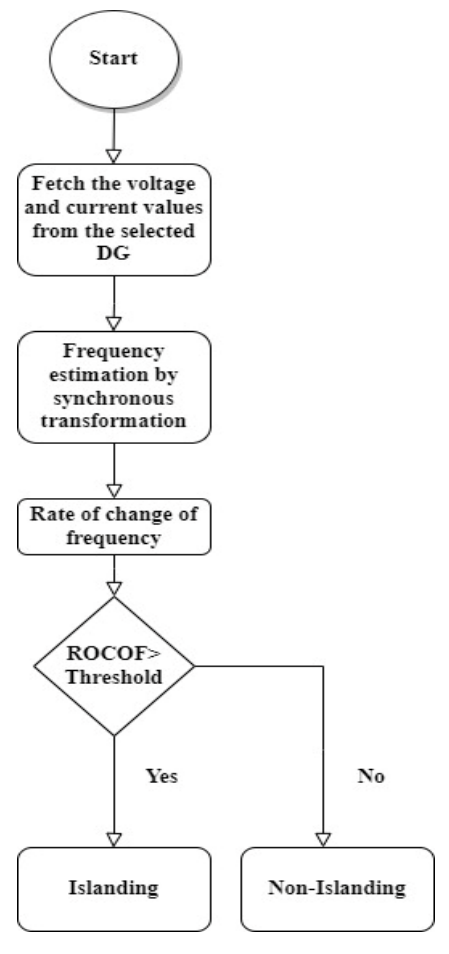


Fig. 1. Flowchart of ROCOF relay.

In the 3PSF for ROCPAD approach, the angle is first calculated, then the ROCPAD is evaluated, and if it exceeds the threshold, islanding occurs. The current and voltage measurements at the intended DG are followed by phase approximation by the 3PSF algorithm depicted in Fig. 2.

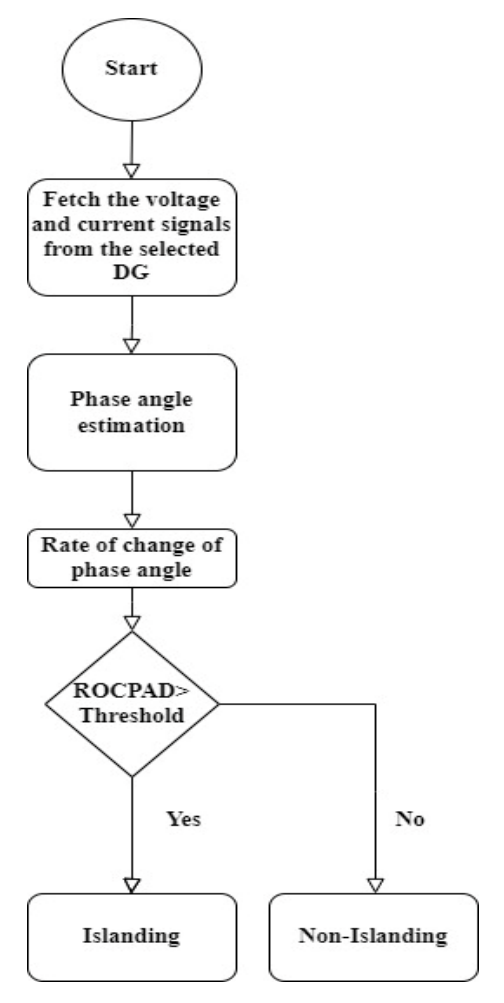


Fig. 2. The 3PSF flowchart for estimating ROCPAD.

3. TEST SYSTEM

The system under examination is depicted in Fig. 3. There is a 10 MVA base power. The system under evaluation includes of four DG units—one emergency diesel generator and three wind farms—that connect a system of radial distribution to the primary grid PCC. The microgrid runs at a voltage of 25 kV, and the DG units are 20 km apart. Table 1 displays the specifics of the requirements for the distribution lines, loads, transformers, generators, and DGs [31].

4. RESULTS AND DISCUSSION

Although the most popular islanding identification system is ROCOF technique available today, it is unavoidably limited in that it cannot identify islanding where there are power imbalances of less than 15%, making it an unreliable relay in situations with modest power mismatches. In the instance of ROCOF, the islanding is carried out at t=3 seconds by activating the circuit breaker (CB)-2 and setting the threshold to be 1.2 Hz/sec. The high power and low power imbalances are seen in Figs. 4 and 5, correspondingly.

Table 1: Transformers, generators, distribution lines (DL),
loads, and DG specifications

Equipment	Description
Generator	$MVA = 1000, V_{base} = 120KV,$ rated $kV = 120$, $f = 50Hz$
Distributed Generators: DG1, DG2, DG3, DG4	1.5 MW wind turbines. 5MW, 400V Emergency Diesel Generator
Transformers: TR-1	$\begin{aligned} MVA &= 50 \text{ , } f = 50 \text{ Hz, rated kV} = \\ 120/25, V_{base} &= 25 \text{ kV, } R_1 = \\ 0.00375 pu, X_1 &= 0.1 \text{ pu, } R_m = 500 \\ pu, X_m &= 500 pu \end{aligned}$
TR-2, TR-3, TR-4 and TR-5	$\begin{array}{l} MVA = 10 \;,\; f = 50 \; Hz, \; rated \; kV = \\ 575/25, \; V_{base} = 25 \; kV, \; R_1 = \\ 0.00375pu, \; X_1 = 0.1 \; pu, \; R_m = 500 \\ pu, \; X_m = 500pu \end{array}$
Distribution lines: DL-1,DL-2, DL-3 and DL-4	$\begin{aligned} & \text{Pi-section 20km each , rated KV} = \\ & 25, \text{MVA} = 20, \text{V}_{\text{base}} = 25 \text{KV}, \end{aligned}$
	$R_o = 0.1153 \text{ ohms/km}, R_1 = 0.413 $ ohms/km
	$L_0 = 1.05e-3 \text{ H/km}$, $L_1 = 3.32e-3$ H/km
	$C_0 = 11.33e-009 \text{ F/km}, C_1 = 5.01e-009\text{F/km}$
Loading: L1, L2, L3, L4, L5	15MW, 5Mvar 8MW, 3Mvar
, , -	olvi vv , sivi vai

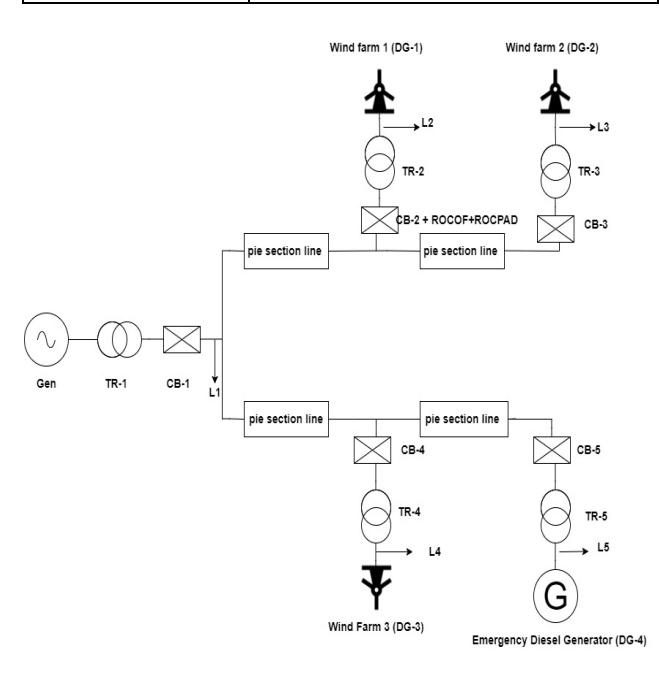


Fig. 3. Schematic illustration of test system.

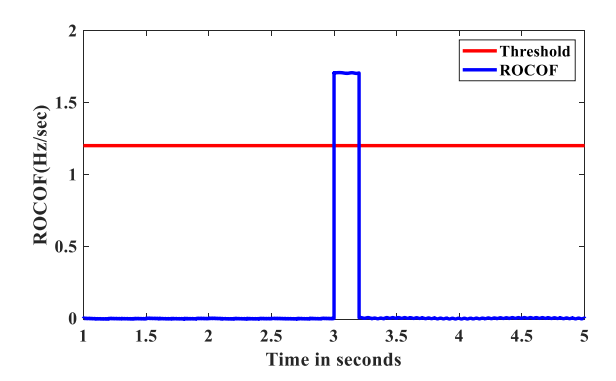


Fig. 4. The execution of ROCOF under islanding detection at DG-1 for high power mismatch.

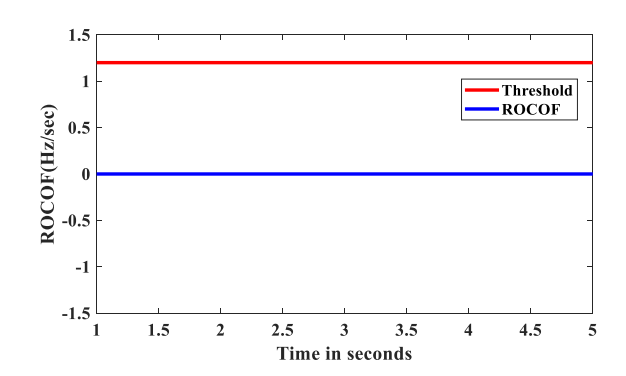


Fig. 5. The execution of ROCOF for islanding detection at DG-1 for low power mismatch.

It is observed from Fig.4 and Fig.5 that the islanding detection is identified for high power imbalance only not for the low power mismatch since it stays below the threshold value. On the other hand, it is clearly observed that Under these settings, that is, the immediate, delay-free detection of islanding for both high and low (zero) power mismatch situations, as shown in Figs. 6 and 7, the proposed 3PSF for ROCPAD functions well.

Here the threshold for ROCPAD is set at 120 Deg/sec.

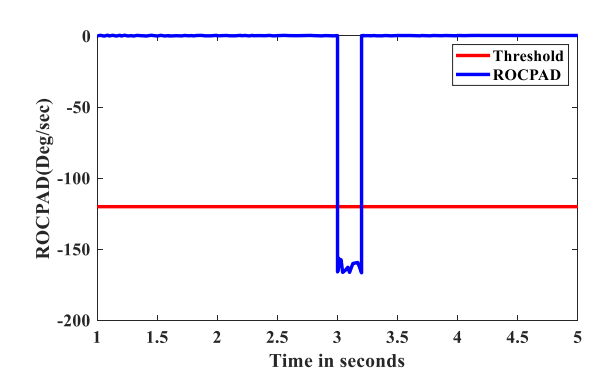


Fig. 6. The execution of 3PSF for ROCPAD in islanding detection at DG-1 for high power mismatch.

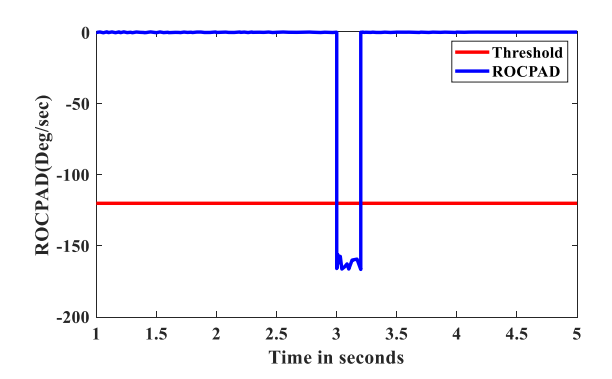


Fig. 7 The execution of 3PSF for ROCPAD in islanding detection at DG-1 for low power (zero) mismatch

The suggested ROCOF and ROCPAD are put under test for the severe 3-phase short circuit fault. The symmetrical 3-phase fault is purposefully created on DG1 at t=3.5 sec, for which Fig. 8 displays the frequency deviation. Frequency variation has been found to be within the acceptable range. Consequently, islanding will not occur in the suggested 3 PSF ROCPAD approach, but the ROCOF relay mal operated for the fault which is displayed in Fig.9 but the 3PSF-ROCPAD did not cross the threshold shown in Fig.10. So it does not give the mal-operation.

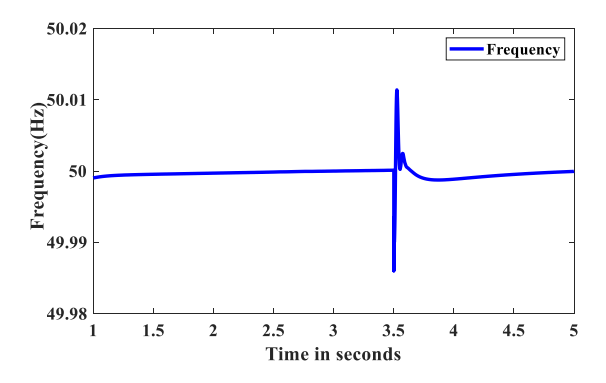


Fig. 8. The frequency characteristics in 3-phase short circuit condition.

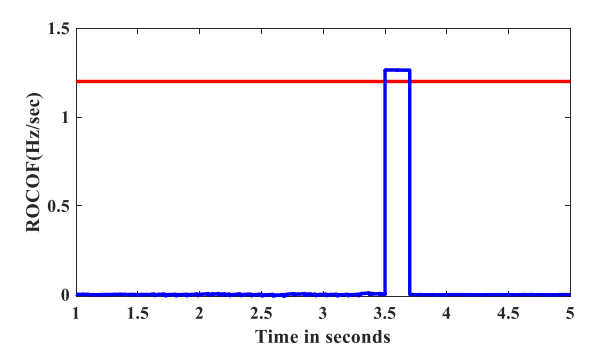


Fig. 9. The execution of ROCOF at 3-phase short circuit fault condition

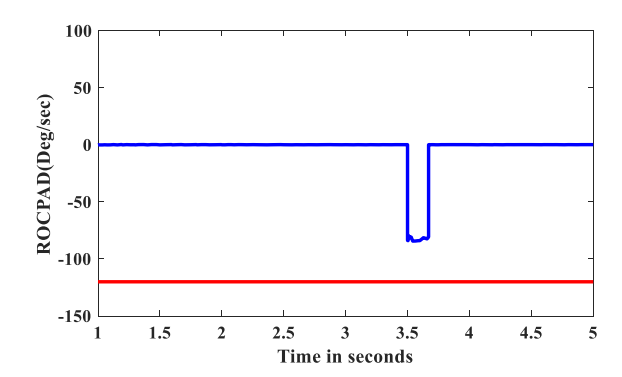


Fig. 10 The execution of 3PSF for ROCPAD at 3-phase short circuit fault condition.

Voltage sags and swells disrupt power systems by compromising the stability and reliability of electrical supply. Sags, characterized by brief voltage reductions, can lead to equipment malfunction, motor torque dips, and visible light flickering, affecting industrial processes and sensitive electronics. Conversely, swells, marked by temporary voltage increases, pose risks of equipment damage, overheating, and insulation breakdown due to excessive voltage. Both disturbances can cause system-wide disruptions, equipment failures, and safety hazards, necessitating the implementation of protective measures. In order to mitigate these issues, the performances of the proposed technique are studied which can detect the voltage sag and swell. The results are depicted in Fig. 11- Fig. 19. In the system the voltage swell and the voltage sag is purposefully created from 1.5 sec to 2.5 sec.

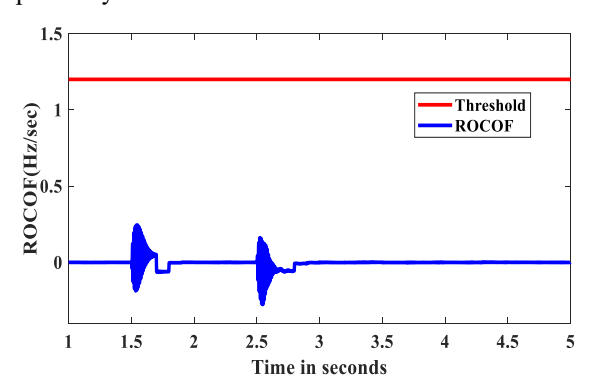


Fig. 11. The execution of ROCOF for 10% voltage sag.

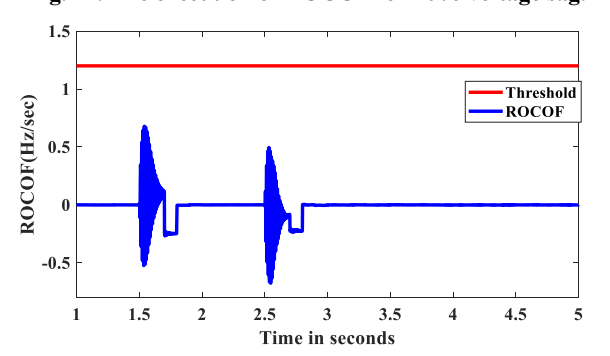


Fig .12. The execution of ROCOF for 20% voltage sag.

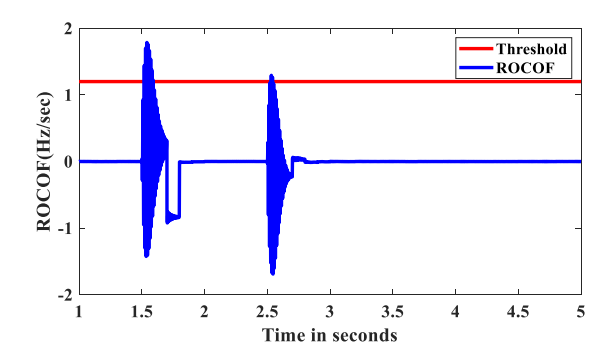


Fig. 13. The execution of ROCOF for 30% voltage sag.

From fig. 11 to fig.13 the performance of the ROCOF is checked for voltage sag It is readily seen that the ROCOF detects islanding at 30% voltage sag since it crosses the threshold value whereas does not detect islanding either at 10% or at 20% since it stays below the threshold value.

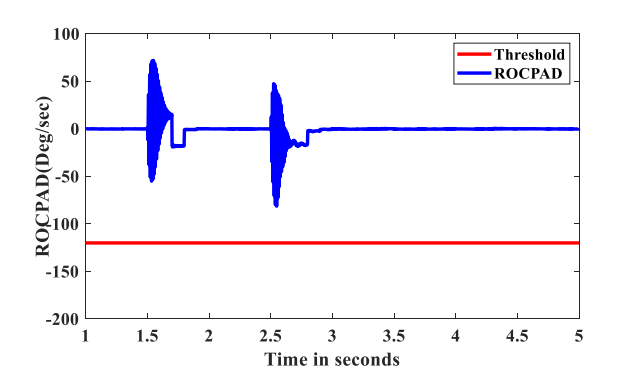


Fig. 14. The execution of ROCPAD for 10% voltage sag.

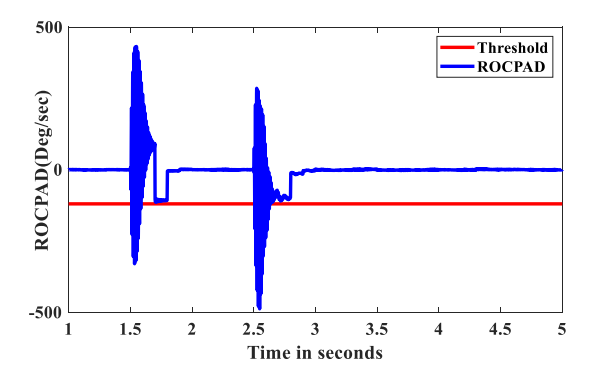


Fig. 15. The execution of ROCPAD for 20% voltage sag.

Through fig.14 and fig.15 the performance of the 3PSF based ROCPAD is checked for voltage sag and it is readily seen that the 3PSF-ROCPAD detects islanding at 20% voltage sag since it crosses the threshold. However it does not detect islanding at 10% voltage sag since it does not cross the threshold. The sensitivity of 3PSF-ROCPAD is found better as compared to ROCOF.

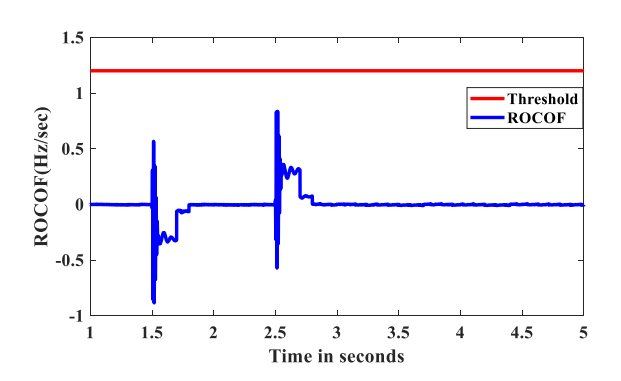


Fig. 16. The execution of ROCOF for 10% voltage swell.

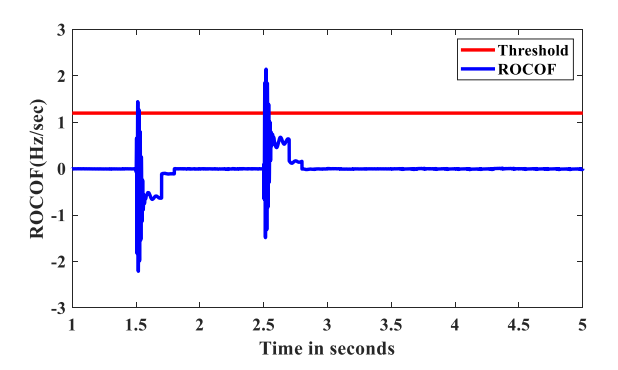


Fig. 17. The execution of ROCOF for 20% voltage swell.

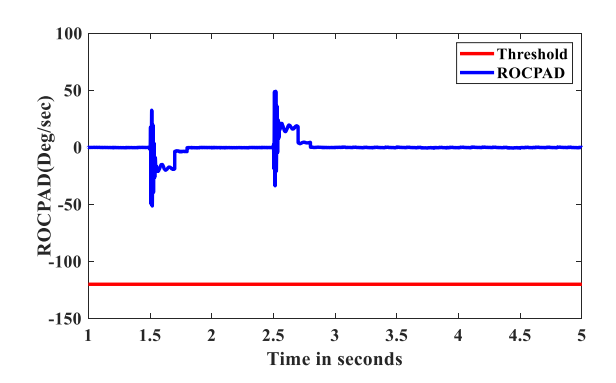


Fig. 18. The execution of ROCPAD for 10% voltage swell.

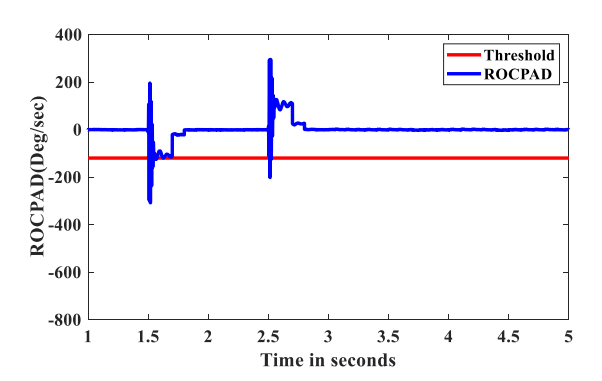


Fig. 19. The execution of ROCPAD for 20% voltage swell.

From fig. 16 and fig.17 the performance of the ROCOF is checked for voltage swell and observations clearly show

that detection is identified at 20% voltage swell.

Similarly, the performance of the ROCPAD is checked for voltage swell shown in Fig. 18 and Fig.19, and observations clearly show that the detection is identified at 20% voltage swell condition.

5. CONCLUSION

The proposed 3PSF approach in a 0% power mismatch scenario instantly detects islanding. The approach prevents the mal-operation of the relay under grid disturbance or short circuit. The proposed algorithm predicted the islanding detection in case of voltage sag/swell conditions. The sag/swell condition was extensively explored. It has been concluded that ROCPAD detects islanding if the voltage sag is below 20% of nominal voltage; whereas ROCOF detects islanding if voltage sag is less than 30% of nominal voltage. Similarly, the islanding detection is identified for the voltage swell if the voltage level exceeding 20% of voltage under ROCOF and ROCPAD, respectively. So it is concluded that the proposed technique is more sensitive and can be used to predict the voltage sag and swell, which improves the reliability of the system. The effectiveness of the suggested algorithm 3PSF obtained superior results to conventional ROCOF. The instantaneous detection of islanding in the all the cases ensuring the reliability of power system.

ACKNOWLEDGMENTS

The authors express their gratitude to Mr. Pushkar Praveen (GBPIET, Pauri Garhwal, Uttarakhand, India) and Dr. Manoj Kumar Panda (Director, WIT Dehradun, Uttarakhand, India) for their insightful remarks and recommendations. Further, this work is going to be extended for the unbalances, interruptions, fluctuations, and flickering.

REFERENCES

- Basso, T.; DeBlasio, R. IEEE 1547 Series of Standards: Interconnection Issues. IEEE Trans. Power Electron. 2004, 19, 1159–1162.
- [2] Etxegarai, A., Eguía, P., & Zamora, I. (2011, April). Analysis of remote islanding detection methods for distributed resources. In *Int. conf. Renew. Energies power quality* (Vol. 1, No. 9).
- [3] Bratton, R. E. (1984). Transfer-trip relaying over a digitally multiplexed fiber optic link. *IEEE transactions on power* apparatus and systems, (2), 403-406.
- [4] Redfern, M. A., Barrett, J., & Usta, O. (1995). A new microprocessor based islanding protection algorithm for dispersed storage and generation units. *IEEE Transactions* on Power Delivery, 10(3), 1249-1254.
- [5] Ropp, M. E., Aaker, K., Haigh, J., & Sabbah, N. (2000, September). Using power line carrier communications to prevent islanding [of PV power systems]. In Conference Record of the Twenty-Eighth IEEE Photovoltaic Specialists Conference-2000 (Cat. No. 00CH37036) (pp. 1675-1678). IEEE.

- [6] Xu, W., Zhang, G., Li, C., Wang, W., Wang, G., & Kliber, J. (2007). A power line signaling based technique for antiislanding protection of distributed generators—Part I: Scheme and analysis. *IEEE Transactions on Power Delivery*, 22(3), 1758-1766.
- [7] Prakash, S., Purwar, S., & Mohanty, S. R. (2020). Adaptive detection of islanding and power quality disturbances in a grid-integrated photovoltaic system. Arabian Journal for Science and Engineering, 45(8), 6297-631.
- [8] Bejmert, D., & Sidhu, T. S. (2014). Investigation into islanding detection with capacitor insertion-based method. *IEEE Transactions on Power Delivery*, 29(6), 2485-2492.
- [9] Rostami, A., Abdi, H., Moradi, M., Olamaei, J., & Naderi, E. (2017). Islanding detection based on ROCOV and ROCORP parameters in the presence of synchronous DG applying the capacitor connection strategy. *Electric Power Components* and Systems, 45(3), 315-330.
- [10] Wen, B., Boroyevich, D., Burgos, R., Shen, Z., & Mattavelli, P. (2015). Impedance-based analysis of active frequency drift islanding detection for grid-tied inverter system. *IEEE Transactions on industry applications*, 52(1), 332-341.
- [11] Voglitsis, D., Papanikolaou, N., & Kyritsis, A. C. (2016). Incorporation of harmonic injection in an interleaved flyback inverter for the implementation of an active anti-islanding technique. *IEEE Transactions on Power Electronics*, 32(11), 8526-8543.
- [12] Azim, R., Li, F., Xue, Y., Starke, M., & Wang, H. (2017). An islanding detection methodology combining decision trees and Sandia frequency shift for inverter-based distributed generations. *IET Generation, Transmission & Distribution*, 11(16), 4104-4113.
- [13] Sun, Q., Guerrero, J. M., Jing, T., Vasquez, J. C., & Yang, R. (2015). An islanding detection method by using frequency positive feedback based on FLL for single-phase microgrid. *IEEE Transactions on Smart Grid*, 8(4), 1821-1830
- [14] Emadi, A., Afrakhte, H., & Sadeh, J. (2016). Fast active islanding detection method based on second harmonic drifting for inverter-based distributed generation. *IET Generation, Transmission & Distribution*, 10(14), 3470-3480.
- [15] Liu, M., Zhao, W., Wang, Q., Huang, S., & Shi, K. (2019). Compatibility issues with irregular current injection islanding detection methods and a solution. *Energies*, 12(8), 1467.
- [16] Du, P., Nelson, J. K., & Ye, Z. (2005). Active anti-islanding schemes for synchronous-machine-based distributed generators. *IEE Proceedings-Generation, Transmission and Distribution*, 152(5), 597-606.
- [17] Roscoe, A. J., Burt, G. M., & Bright, C. G. (2014). Avoiding the non-detection zone of passive loss-of-mains (islanding) relays for synchronous generation by using low bandwidth control loops and controlled reactive power mismatches. *IEEE Transactions on smart grid*, 5(2), 602-611
- [18] Zamani, R., Hamedani-Golshan, M. E., Haes Alhelou, H., Siano, P., & R. Pota, H. (2018). Islanding detection of synchronous distributed generator based on the active and reactive power control loops. *Energies*, 11(10), 2819.
- [19] Tan, K. H., & Lan, C. W. (2019). DG system using PFNN

- controllers for improving islanding detection and power control. *Energies*, 12(3), 506.
- [20] Vieira, J. C., Freitas, W., Xu, W., & Morelato, A. (2008). An investigation on the nondetection zones of synchronous distributed generation anti-islanding protection. *IEEE* transactions on power delivery, 23(2), 593-600.
- [21] Pigazo, A., Liserre, M., Mastromauro, R. A., Moreno, V. M., & Dell'Aquila, A. (2008). Wavelet-based islanding detection in grid-connected PV systems. *IEEE Transactions on Industrial Electronics*, 56(11), 4445-4455.
- [22] Ning, J., & Wang, C. (2012, July). Feature extraction for islanding detection using Wavelet Transform-based Multi-Resolution Analysis. In 2012 IEEE Power and Energy Society General Meeting (pp. 1-6). IEEE.
- [23] Zamani, R., & Golshan, M. E. H. (2018, April). Islanding detection of synchronous machine-based distributed generators using signal trajectory pattern recognition. In 2018 6th International Istanbul Smart Grids and Cities Congress and Fair (ICSG) (pp. 91-95). IEEE.
- [24] Liu, X., Zheng, X., He, Y., Zeng, G., & Zhou, Y. (2019). Passive islanding detection method for grid-connected inverters based on closed-loop frequency control. *Journal of Electrical Engineering & Technology*, 14, 2323-2332.
- [25] Abd-Elkader, A. G., Saleh, S. M., & Eiteba, M. M. (2018). A passive islanding detection strategy for multi-distributed generations. *International Journal of Electrical Power & Energy Systems*, 99, 146-155.
- [26] Bezawada, P., Yeddula, P. O., & Kota, V. R. (2021). A novel time-domain passive islanding detection technique for gridconnected hybrid distributed generation system. Arabian

- Journal for Science and Engineering, 46, 9867-9877.
- [27] Kong, X., Xu, X., Yan, Z., Chen, S., Yang, H., & Han, D. (2018). Deep learning hybrid method for islanding detection in distributed generation. *Applied Energy*, 210, 776-785.
- [28] Kumar, M., & Kumar, J. (2023). A Solution to Islanding Event Detection Using Superimposed Negative Sequence Components-Based Scheme. Arabian Journal for Science and Engineering, 1-15.
- [29] Bhatt, N., & Kumar, A. (2020). A passive islanding detection algorithm based on modal current and adaptive boosting. Arabian Journal for Science and Engineering, 45, 6791-6801.
- [30] Abyaz, A., Panahi, H., Zamani, R., Haes Alhelou, H., Siano, P., Shafie-Khah, M., & Parente, M. (2019). An effective passive islanding detection algorithm for distributed generations. *Energies*, 12(16), 3160.
- [31] Samui, A.; Samantaray, S.R. Assessment of ROCPAD Relay for Islanding Detection in Distributed Generation. IEEE Trans. Smart Grid 2011, 2, 391–398.
- [32] Patcharaprakiti, N., Tunlasakun, K., Kirtikara, K., Chenvidhya, D., Monyakul, V., Jivacate, C., ... & Thongpron, J. Modeling of Islanding Detection for Inverter-Based Distributed Generator using Nonlinear System Identification Approach.
- [33] Pachanapan, P. (2018). Islanding management of microgrid with multi-renewable energy sources. GMSARN Int. J, 12, 47-55.
- [34] Pachanapan, P., & Premrudeepreechacharn, S. (2020). Dynamic Performances of Multi-Renewable Energy Sources in a MicrogridDuring Islanding Operation.